Radiotherapy and Oncology 205 (2025) 110762

Contents lists available at ScienceDirect

Radiotherapy and Oncology

journal homepage: www.thegreenjournal.com

Original Article

# Synthetic CT generation using Zero TE MR for head-and-neck radiotherapy

Iris Lauwers [a,*], Marta Capala [a], Sandeep Kaushik [b,c], László Ruskó [d], Cristina Cozzini [b], Jean-Paul Kleijnen [e], Jonathan Wyatt [f,g], Hazel McCallum [f,g], Gerda Verduijn [a], Florian Wiesinger [b], Juan Hernandez-Tamames [h,i], Steven Petit [a]

[a] Department of Radiotherapy, Erasmus MC Cancer Institute, University Medical Center Rotterdam, Rotterdam, the Netherlands
[b] GE HealthCare, Munich, Germany
[c] Department of Quantitative Biomedicine, University of Zurich, Zurich, Switzerland
[d] GE Healthcare Magyarország Kft., Budapest, Hungary
[e] Department of Medical Physics, Haaglanden MC, The Hague, the Netherlands
[f] Translational and Clinical Research Institute, Newcastle University, Newcastle, UK
[g] Northern Centre for Cancer Care, Newcastle upon Tyne Hospitals NHS Foundation Trust, Newcastle, UK
[h] Department of Radiology and Nuclear Medicine, Erasmus MC, Rotterdam, the Netherlands
[i] Department of Imaging Physics, TU Delft, Delft, the Netherlands

ARTICLE INFO

*Keywords:*
MROnly
Zero TE MRI
ZTE
Synthetic CT
Head and neck

ABSTRACT

*Background and Purpose:* MRI-based synthetic CTs (synCTs) show promise to replace planning CT scans in various anatomical regions. However, the head-and-neck region remains challenging because of patient-specific air, bone and soft tissues interfaces and oropharynx cavities. Zero-Echo-Time (ZTE) MRI can be fast and silent, accurately discriminate bone and air, and could potentially lead to high dose calculation accuracy, but is relatively unexplored for the head-and-neck region. Here, we prospectively evaluated the dosimetric accuracy of a novel, fast ZTE sequence for synCT generation.

*Materials and Methods:* The method was developed based on 127 patients and validated in an independent test (n = 17). synCTs were generated using a multi-task 2D U-net from ZTE MRIs (scanning time: 2:33 min (normal scan) or 56 s (accelerated scan)). Clinical treatment plans were recalculated on the synCT. The Hounsfield Units (HU) and dose-volume-histogram metrics were compared between the synCT and CT. Subsequently, synthetic treatment plans were generated to systematically assess dosimetry accuracy in different anatomical regions using dose-volume-histogram metrics.

*Results:* The mean absolute error between the synCT and CT was 94 ± 11 HU inside the patient contour. For the clinical plans, 98.8% of PTV metrics deviated less than 2% between synCT and CT and all OAR metrics deviated less than 1 Gy. The synthetic plans showed larger dose differences depending on the location of the PTV.

*Conclusions:* Excellent dose agreement was found based on clinical plans between the CT and a ZTE-MR-based synCT in the head-and-neck region. Synthetic plans are an important addition to clinical plans to evaluate the dosimetric accuracy of synCT scans.

## Introduction

In head-and-neck (HN) radiotherapy, magnetic resonance imaging (MRI) is often used to accurately delineate because of its superior soft tissue contrast compared to computed tomography (CT). A CT scan is required to provide the tissue electron density for dose calculations. However, using two imaging modalities brings along several challenges: MR and CT images have to be registered which induces a registration uncertainty; it might delay the start of treatment; it increases the overall treatment preparation costs and workload; and acquiring a CT leads to more concomitant dose received by the patient [1–6]. Moreover, the need for a CT limits the benefits of adaptive real-time MR-guided radiotherapy treatment adaption *e.g.* using a MRI-linac system [2,7]. These challenges and limitations could be overcome by using an MR-only radiotherapy workflow.

The HN region remains challenging for deep-learning-based

* Corresponding author at: Department of Radiotherapy, Erasmus MC Cancer Institute, P.O. Box 2040, 3000 CA Rotterdam, the Netherlands.
*E-mail address:* i.lauwers@erasmusmc.nl (I. Lauwers).

https://doi.org/10.1016/j.radonc.2025.110762
Received 16 August 2024; Received in revised form 16 December 2024; Accepted 27 January 2025
Available online 29 January 2025

synthetic CT-(synCT)-generation due to complex anatomical localization and large anatomical heterogeneity with many bony structures. These bony structures provide a similar MR signal as air due to their low water content and short signal lifetimes, while the Hounsfield Units (HU) of bone and water greatly differ [1,2,8,9]. Prior studies proposed using multiple time-expensive MR sequences for synCT generation. For instance, Qi et al. concluded that combining a T1 weighted, T2 weighted, T1 contrast, and T1 Dixon contrast scan improved the synCT accuracy and Palmér et al. showed excellent dosimetric results based on a T1 weighted Dixon Vibe MRI, which took ~10 min to acquire [10,11]. However, any additional time required for MR-only workflow based sequences should be minimized, as patients are typically scanned in immobilization masks that are considered uncomfortable and long scanning times can introduce more intra scanning motion [2].

In recent years, Zero-echo-time (ZTE) MRI has been developed. This sequence can be made silent, is relatively fast, might give a relevant bone signal, and, unlike the often-used DIXON scans, it enables couch segmentation that is needed for dose planning and optimalisation [9,12]. ZTE MRI has been successfully used in synCT generation for other sites, such as the pelvis and brain [13–15]; however, to the best of our knowledge, it has not been extensively or exclusively explored for the HN region. Although Bambach et al. included ZTE MRI for synCT generation in the HN region, they did not perform dosimetric evaluations. Moreover, they investigated bone MRI sequences in general (gradient recalled-echo, ultrashort-TE, and ZTE sequences) and the ZTE MRIs specific results were not separately reported on [16]. Therefore, the potential of ZTE-based synCTs remains unclear.

The goal of the current prospective study was to investigate the HU and dosimetric accuracy of radiotherapy dose calculations of synCT scan of the HN region based on a multi-task 2D U-net and fast ZTE-sequences, to be acquired in preferably less than one minute. In addition to the clinical treatment plans, synthetic treatments plans were created to systematically assess the dosimetric accuracy in extreme situations across a range of anatomical locations within the HN region.

## Materials and methods

### *Patients and treatment*

This current research was part of the *Deep learning based MR Only Radiotherapy for head-and-neck cancer* clinical study approved by the Erasmus MC Institution Review Board [MEC-2019–0805] [17]. The inclusion criteria consisted of HN cancer patients who underwent a planning MRI for radiotherapy and were at least eighteen years old. The exclusion criteria included any physical or mental health condition that interfered with the informed consent process or any contraindications for MRI, such as claustrophobia or arterial clips in the central nervous system. For MRI sequence optimization, training, and development of the synCT method, 127 patient datasets (including N = 24 from Erasmus MC) were used. A separate set (N = 19) HN patients that were treated consecutively between January 2022 and July 2024 at Erasmus MC were included as test set to investigate the HU accuracy of the synCT scans and to evaluate the suitability for radiotherapy dose calculations.

### *CT and MRI scanning*

Before start of treatment, planning CT (planCT) scans were acquired in treatment position with a radiotherapy immobilization mask according to clinical practice on locally available CT scanners. In case of Erasmus MC, a Siemens SOMATOM Confidence (Siemens Healthineers, Erlangen, Germany) was used. Next, patients were scanned in treatment position with a radiotherapy immobilization mask on a 1.5 T GE MR450w using the GEM RT Head & Neck coil suite (GE HealthCare, Chicago, IL). In Erasmus MC, the 3D radial ZTE sequence was acquired with a field of view = 50x50x37.5 $cm^3$, resolution = 250 slices, spatial resolution = 1.6x1.6x1.5 $mm^3$, flip angle = 1 deg, imaging bandwidth =±100 kHz, number of averages (NEX) = 1.5, and scan time = 2min33sec [18,19]. For the training set ZTE images that were not acquired at Erasmus MC, the MR ZTE protocol was kept identical regarding main scan parameter (*e.g.* FOV, resolution, FA, and BW); however, some aspects differed per site (*e.g.* coil configuration and scan time).

For six out of the last seven patients, an accelerated version of the original ZTE protocol was tested with a 56sec (res = 2.0x2.0x2.0 $mm^3$, NEX = 1) scan time.

### *Training the model for synthetic CT generation*

To convert ZTE MR scans to synCT scans, a method was applied that was described in [13]. In short, the preprocessing involved N4 inhomogeneity correction for the MR images, normalization to [-1000, 3000] for the CT, and Z-score normalization for the ZTE images. The method consists of a multi-task 2D U-net with weighted losses. The loss function was a combination of the mean absolute error (MAE) in the patient, the MAE in the bone region, and the Dice in the bone region. Thresholding was used to define the bone region. Before training the planCT images were non-rigidly registered to ZTE images covering the brain, head-neck, and shoulder anatomies, using the mutual information metric and symmetric normalization implemented by ITK-ANTs libraries for an improved alignment between the two images. More details about the synCT generation can be found in [13].

### *Applying synthetic CT generation for the patients in the test set*

The above-described deep-learning-based ZTE to synthetic CT image translation was applied to the test set. To facilitate the dosimetric comparison the synCT scans were non-rigidly deformed to the planCT scans, to avoid the effect of any anatomical/positioning differences between the planCT and the synCT. The clinical HU to relative electron density calibration curve was used for both the synCT and planCT (Supplementary information A).

### *Hounsfield units comparison*

For the HU analysis, the patient contour was reduced by 2 cm to exclude the patient edges that were often influenced by registration inaccuracies. The effect of the 2 mm reduction was assessed in Supplementary Information table B1 and deemed neglectable compared to *e.g.* 1 cm. Moreover, the patient contour was cropped from the top of the sternum to the middle of the brain for consistency over the patient cohort. Or in cases where the scan did not reach from the sternum to the middle of the brain, it was cropped to the highest and lowest slice with a complete signal.

The HU were compared between the synCT and planCT in the test set using the MAE and mean error (ME) within the adapted patient contour. The accuracy of different tissue classes (*i.e.*, air, soft tissue and bone) was separately assessed using the MAE and Dice similarity coefficient. Air, soft-tissue and bone regions were identified using the following thresholding conditions $HU_{air} < -250$ HU $< HU_{soft\text{-}tissue} < 200$ HU $< HU_{bone}$.

### *Clinical treatment plans and dosimetric comparison*

All patients were treated according to standard clinical practice using Volumetric-Modulated Arc Therapy (VMAT). Treatment planning was performed using Monaco 6.00.01 (Elekta AB, Stockholm, Sweden). The prescribed dose varied between 59 and 70 Gy and was delivered in 20 to 35 fractions.

The clinical contours of organs and risk (OARs) and planning target volume (PTV) were projected on the synCT, that was deformably registered to the planCT, as described above. Next, the clinical treatment plan was recalculated on the planCT and the synCT using the Monte Carlo dose algorithm of Scimoca 1.5.0.2821 (ScientificRT GmbH,

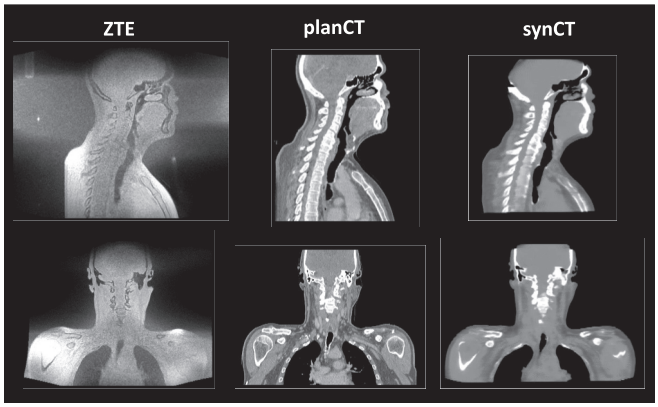


**Fig. 1.** An example of (from left to right) the 2:33 min Zero echo time (ZTE) MRI, the planning CT (planCT) and the synthetic CT (synCT) in the sagittal (top) and coronal (bottom) view.

Munich, Germany) with a 2x2x2 mm grid spacing and a computational uncertainty of 0.5% ("extra fine"). Scimoca was used as it allows to recalculate the clinical plans with high accuracy in batch processing mode on both the planCT and synCT. The dose distributions on the planCT and synCT were compared using the following dose metrics: Dmean for the parallel OARs, near maximum dose (D2%) for the serial OARs, and Dmean, near maximum dose (D2%), and near minimal dose (D98%) for the PTVs. Also, population dose volume histograms (DVHs) were calculated and global gamma (2%/2mm and 1%/1mm) calculations with a minimum cut-off value of 10% of the prescribed dose to the high-dose PTV were calculated.

*Synthetic treatment plans and dosimetric comparison*

Using the clinical treatment plans for evaluation of dosimetric accuracy is clinically meaningful. However, this dosimetric accuracy is only evaluated for a limited part of the patient anatomy. Moreover, VMAT plans that deliver radiation from a large number of directions tend to be forgiving for small HU inaccuracies. Therefore, a second dosimetric comparison was performed using synthetic plans.

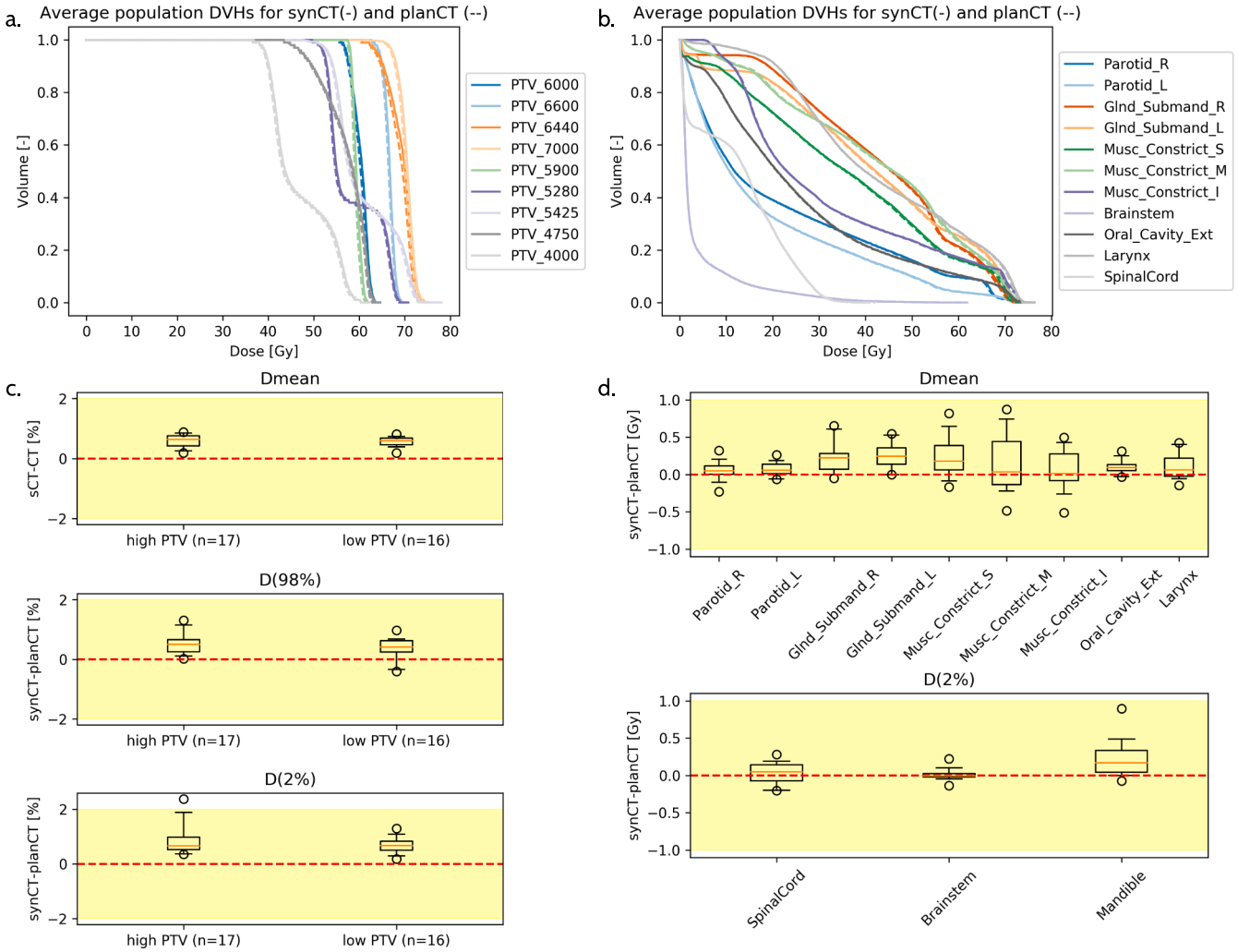


**Fig. 2.** The dose volume histogram (DVH) comparison between the planning CT (planCT) and the synthetic CT (synCT) based on clinical plans. a). The average population DVH of the planning target volumes (PTVs) with the synCT doses as solid lines and the planCT doses as dotted lines. b). The population DVH of the organs at risk (OAR) of the planning target volumes (PTVs) with the synCT doses as solid lines and the planCT doses as dotted lines. c). The difference in DVH metrics for the PTVs from top to bottom: average dose (Dmean), near minimum dose (D(98%)), and near maximum dose (D(2%)) divided in the high dose PTV and low dose PTV. d). The difference in DVH metrics for the OAR from top to bottom: average dose (Dmean) for parallel organs the and near maximum dose (D(2 %)) for serial organs. The red lines represent the medians, the boxes the 25 % to 75 % range, the whiskers the 5% to 95% range, and the circles datapoint outside of the range of the whiskers. The yellow plane marks the clinically acceptable range: 2% or 1 Gy. (For interpretation of the references to colour in this figure legend, the reader is referred to the web version of this article.)

**Table 1**
The mean and standard deviations of the DVH metric' differences over the clinical plans of all patients between the planning and synthetic CT scans for the PTVs (top) and OARs (bottom). A positive difference indicates the DVH metric is higher in the synthetic CT based dose distribution compared to the planning CT based dose distribution.

| PTV DVH metric Structure | Metric | Mean dose difference [Gy] | Mean dose difference [%] |
|---|---|---|---|
| High dose PTV | Dmean | 0.41 ± 0.14 | 0.59 ± 0.20 |
| | D(98 %) | 0.35 ± 0.24 | 0.54 ± 0.35 |
| | D(2 %) | 0.65 ± 0.41 | 0.90 ± 0.56 |
| Low dose PTV | Dmean | 0.33 ± 0.09 | 0.56 ± 0.16 |
| | D(98 %) | 0.18 ± 0.18 | 0.37 ± 0.35 |
| | D(2 %) | 0.47 ± 0.21 | 0.67 ± 0.29 |
| OAR DVH metric Structure | Metric | Mean dose difference [Gy] | Mean dose difference [%] |
| Parotid (right) | Dmean | 0.06 ± 0.12 | 0.07 ± 0.78 |
| Parotid (left) | Dmean | 0.07 ± 0.09 | 0.18 ± 0.83 |
| Submandibular gland (right) | Dmean | 0.23 ± 0.20 | 0.45 ± 0.33 |
| Submandibular gland (left) | Dmean | 0.25 ± 0.16 | 0.57 ± 0.35 |
| Musculus constrictor S | Dmean | 0.24 ± 0.25 | 0.28 ± 1.44 |
| Musculus constrictor M | Dmean | 0.15 ± 0.38 | 0.00 ± 1.20 |
| Musculus constrictor I | Dmean | 0.06 ± 0.27 | 0.50 ± 1.31 |
| Oral cavity | Dmean | 0.10 ± 0.10 | 0.26 ± 0.42 |
| Larynx | Dmean | 0.10 ± 0.17 | 0.21 ± 0.38 |
| Spinal Cord | D(2 %) | 0.03 ± 0.15 | 0.17 ± 0.55 |
| Brainstem | D(2 %) | 0.01 ± 0.07 | −0.02 ± 0.57 |
| Mandible | D(2 %) | 0.22 ± 0.23 | 0.37 ± 0.38 |

PTV = planning target volume; DVH = dose volume histogram; OAR = organ at risk.

Additional synthetic treatment plans were generated consisting of thirty single beams with 3x3 $cm^2$ fields positioned at six beam angles from 0° to 150° with steps of 30° at five different cranial-caudal levels: the top of the sternum, the middle of the neck, the mandible, the nasal cavity, and the brain (see Fig. 3). In case the synCT did not reach until the brain or sternum level, these levels were removed. The isocenters were positioned on a line in cranial-caudal position through the center of mass of the patient contour. The number of monitor units of each beam was set to an arbitrary 33.2 MU. Note that the number of monitor units did not affect the results, as all dose comparisons for the synthetic plan are presented in percentages (see below).

As surrogates for PTVs, synthetic PTVs were generated for each beam. These were spherical volumes of interest (VOIs) with a diameter of 3 cm and were placed at 1 cm intervals starting at 1.5 cm from the entry point of the beam up to the exit point. For each VOI, the following percentage dose metrics differences were compared between synCT and planCT: Dmean, near maximum dose (D2%) and near minimal dose (D98%).

*Data analysis and statistics*

The DVH metrics were compared between the planCT and synCT. The PTV and VOI DVH metrics were deemed acceptable if for 95 % of the PTVs the difference in metric value was less than 2 % [20]. The OAR DVH metrics were deemed acceptable if for 95 % of the patients the difference was within 1 Gy. Unless mentioned otherwise, the results are presented for the normal ZTE acquisitions (2min33sec acquisition time), and otherwise for the accelerated ZTE scans (56sec). The clinical DVH metrics are compared between the synCT and planCT using a Wilcoxon signed-rank test and a Bonferroni correction to correct for multiple testing.

## Results

Nineteen patients were enrolled in the test set of this study. One patient had to be excluded due to a coil defect and for one patient the raw imaging data could not be retrieved. The remaining seventeen patients were used for the HU and dosimetric validation. An example of the ZTE, synCT, and planCT is given in Fig. 1. For six patients also an accelerated ZTE scan (56 sec) was acquired for synCT scan generation. Supplementary Information C shows an example.

The mean MAE and ME and standard deviations between the synCT and planCT were 94 ± 11 HU and +29 ± 11 HU respectively in the adapted total body contour on the test set. In the different tissue types, the MAE was 288 ± 37 HU, 55 ± 7 HU and 186 ± 56 HU in bone tissue, soft tissue, and air respectively. The Dice similarity indices were 0.63 ± 0.06, 0.94 ± 0.01, and 0.87 ± 0.06 for the bone tissue, soft tissue, and air respectively.

The gamma analysis of the clinical plans had an acceptance rate of 96.6 ± 1.7% and 99.6 ± 0.4% for the 1%1mm and 2%2mm respectively. The corresponding population DVHs and the difference in DVH metrics are shown in Fig. 2 and Table 1. For all PTVs, the difference in Dmean and D98% was less than 2%. For 26 out of 27 PTVs (~96.3 %), the D2% metric differed less than 2% between the planCT and synCT. For the patient that did not reach the requirements the high dose was close to the pharynx, whose shaped deviated between the synCT and planCT. For all OARs, the difference in DVH metrics was less than 1 Gy (See Table 1 and Fig. 2). Even though 98.8% of the PTV and 100 % of the OAR metrics reached our clinical constraints, there was a significant difference for all PTV metrics and five out of twelve OAR metrics between the planCT and synCT.

For the last six patients, also accelerated ZTE scan (56 s) were acquired. The average MAE for these six patients were 96.7 ± 5.8 and 107.4 ± 6.3 HU for the normal and accelerated ZTE-based synCT respectively in the adapted total body contour. For the PTV and OAR DVH metrics based on the accelerated ZTE-based synCT 97.2% and 98.6% differed less than 2% and 1 Gy compared to the planning CT respectively (Supplementary information C).

Besides the clinical plans, we evaluated synthetic plans at five beam level and six angles in on average 398 VOIs per patient (Figs. 3 and 4). The minimum and maximum of the average metric differences at the different levels were only 0.09 ± 1.25% and 1.14 ± 4.18%, respectively (see Table 2). The dose based on the synCT was often higher than the dose based on the planCT, causing over 5% of the VOI's DVH metrics to differ more than 2% for each metric and each level, except for the brain level.

Highest DVH deviations were found at top of the sternum level. Manual assessment of the synCTs and planCTs gave possible explanations for the dose differences, namely, registration errors (especially at the lower levels), underestimation of the bone region, and overestimation of the fat layer (see Supplementary information D for an example).

## Discussion

The need for both a CT and an MRI for radiotherapy treatment planning has multiple disadvantages, *e.g.* registration uncertainty, higher workflow complexity and costs, and a delayed start of treatment. In recent years, methods have been developed to create synCTs based on MR images. For the HN region, the optimal MR sequence for synCT generation should be acquired in less than one minute, be silent, accurately distinct bone and air interfaces, and would lead to accurate dose calculations. In this prospective study, we describe and evaluated silent ZTE sequences for the HN region that can be acquired in only 2:33 min and 0:56 min. Both scans could be converted to synCT scans leading to excellent dosimetric accuracy.

The dose metrics for the PTVs and OARs of the clinical plans were in excellent agreement between the synCT and planCT. For the PTVs,

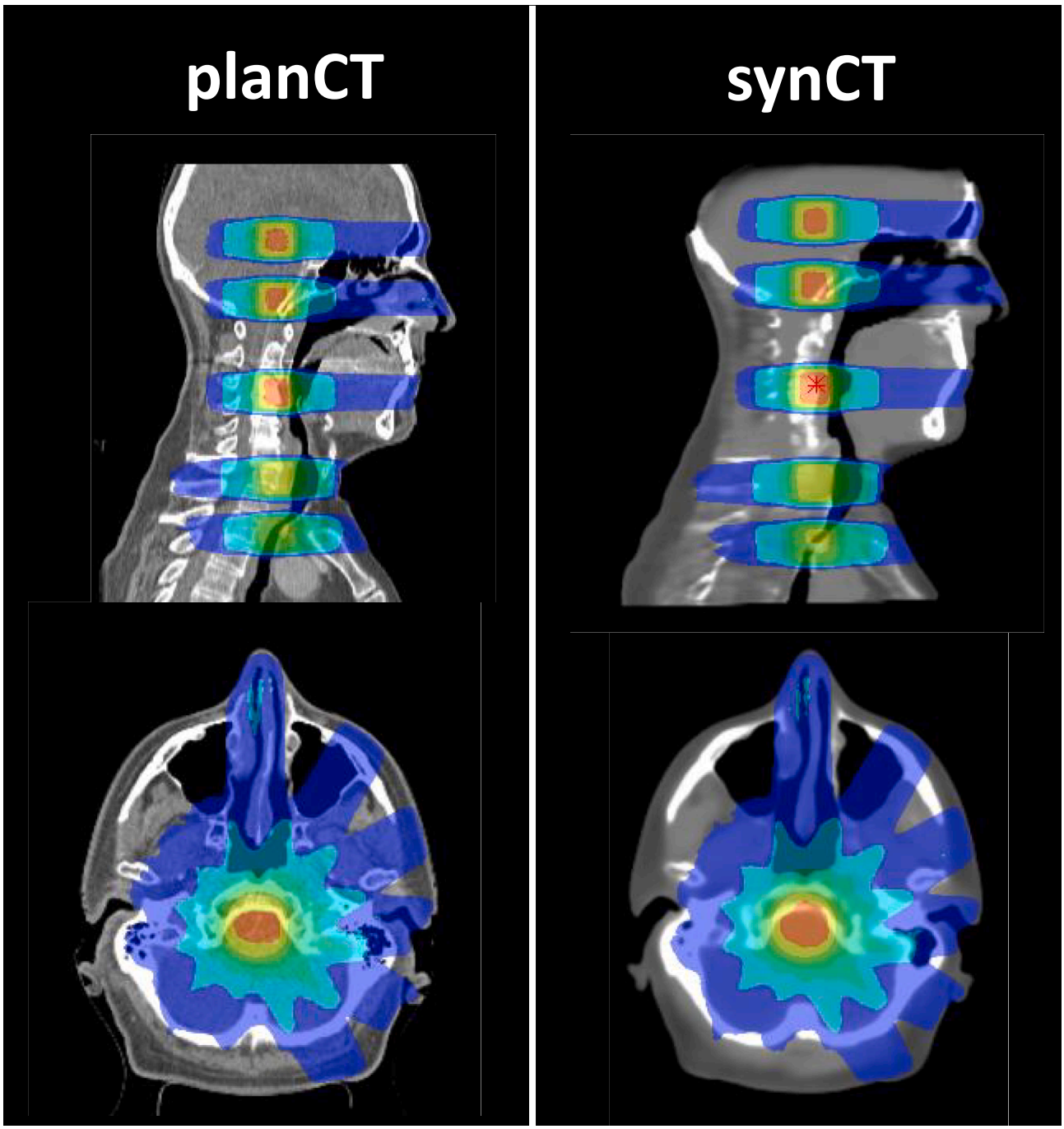


**Fig. 3.** An example of the dose based on the synthetic plans on the planning CT (left) and synthetic CT (right) with from top to bottom the sagittal and axial plane. The synthetic plan contain six beam angles with the same MU at five levels (top of the sternum, middle of the neck, the mandible, the nasal cavity and middle of the brain).

98.8% of PTV metrics deviated less than 2% between synCT and planCT and all dose metrics for the OARs were accurate within 1 Gy. For the accelerated ZTE-based synCTs, 97.2% of the PTV and 98.6% of the OAR metrics were within 2% and 1 Gy respectively. This indicates that the dosimetric results on the synCTs were clinically acceptable [20].

Averaged over the standard ZTE-based synCT of all patients, the average dosimetric error of the synthetic plans was +0.7% on the DVH metrics. For over 5% of the synthetic PTV dose metrics differenced more than 2%, and a systematic error can be seen where the dose in the synCT is slightly though systematically overestimated. This can to a lesser extent also be seen for the clinical plans and is reflected in the positive mean error in HU for all patients and the number of significant dose differences between the synCT and planCT clinicals DVH metrics. Possible causes for the dosimetric deviations are registration errors, underestimation of HU of bone, and overestimation of the fat region. Note that for the clinical VMAT plans, these HU inaccuracies did not lead to clinically relevant errors in dose; but the experiments with the synthetic plans indicate that caution is advised when using limited beam angles. This finding demonstrates the importance of using, in addition to clinical treatment plans, synthetic plans to evaluate the dosimetric accuracy of synCT scans.

The dosimetric accuracy of the clinical results was similar to some of the best performing MR-only methods described in literature (DVH metrics and gamma analysis) [10,11,21–27]. For instance, Olin et al.'s

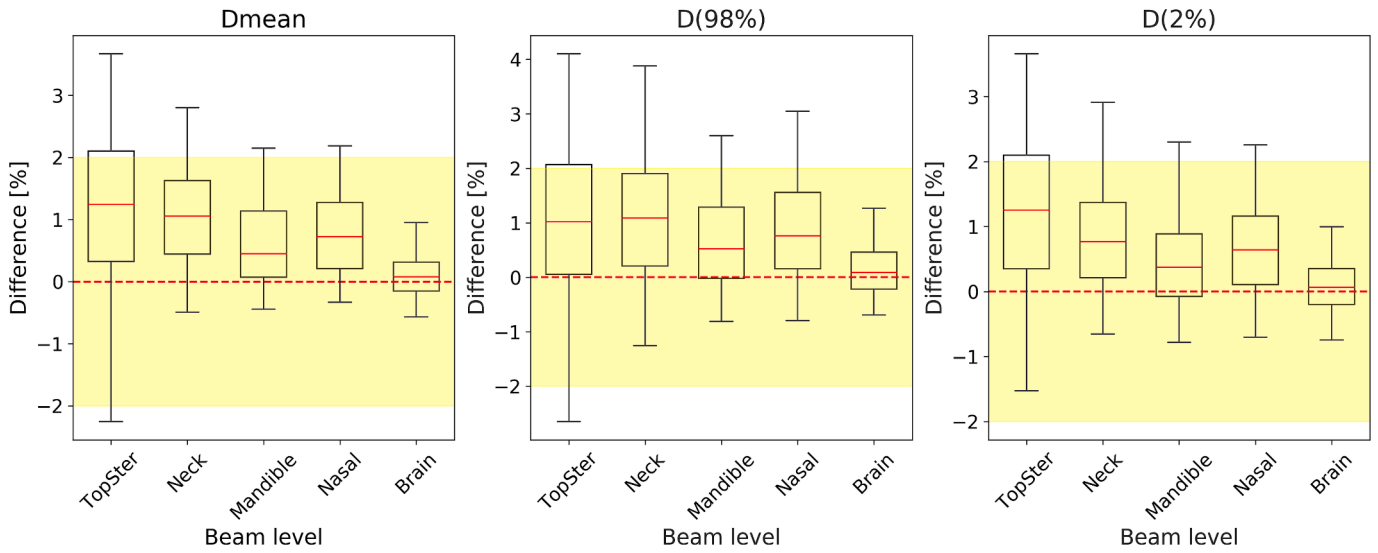


**Fig. 4.** The difference in dose volume histogram metrics for the synthetic planning target volumes for the synthetic plans from left to right: average dose (Dmean), near minimum dose (D98), and near maximum dose (D02). The red lines represent the medians, the boxes the 25% to 75% range and the whiskers the 5% to 95% range. The yellow plane marks the clinically acceptable range (2%). (For interpretation of the references to colour in this figure legend, the reader is referred to the web version of this article.)

**Table 2**
The mean and standard deviations of the DVH metric' differences over all synthetic planning target volumes of all patients between the planning and synthetic CT at different beam levels.

| Beam level | Dmean [%] | D02% [%] | D98% [%] |
|---|---|---|---|
| Top sternum | 1.09 ± 1.78 | 1.15 ± 1.74 | 0.97 ± 2.39 |
| Middle neck | 1.08 ± 1.55 | 0.90 ± 1.41 | 1.14 ± 4.18 |
| Mandible | 0.68 ± 0.82 | 0.51 ± 0.97 | 0.66 ± 1.10 |
| Nasal cavity | 0.78 ± 0.81 | 0.68 ± 0.90 | 0.89 ± 1.23 |
| Brain | 0.11 ± 0.53 | 0.10 ± 0.55 | 0.09 ± 1.25 |

vendor-provided Dixon-sequence-based synCTs also met our clinical requirements although their gamma results are slightly lower than ours [25]. Palmér et al. showed a better dose agreement in terms of DVH metrics between the planCT and their T1-weighted Dixon-Vibe-based synCT than our results. However, they did correct for registration inaccuracies [10]. In our synthetic plans assessment, these registration inaccuracies were identified as one of the main causes of dose disparities. Large differences between methodologies across studies, for instance due to no separate testing sets, small testing sets, different post-processing techniques, and the use of different DVH metrics and less OAR [10,11,21,24,25,28], should be taken into account when comparing different studies.

To the best of our knowledge, this is the first extensive evaluation of ZTE MRI in the HN region for MR-only radiotherapy. This sequence has several benefits. First, the patient comfort, because the sequence can be made silent [19]. Second, the scan can be acquired within only 56 s, as shown for the last six patients. In comparison, the T1 weighted Dixon Vibe scan as acquired by Palmér et al. resulted in very good dose results, but took 9 min 57sec to acquire [10]. The Dixon-based scans described by Olin could also be acquired within a minute, though with different resolution and using a 3 Tesla scanner [24,25]. A third benefit of the ZTE is its ability to differentiate the short-lived MR bone signals from air due to its zero echo time characteristic. This is further explored in Supplementary Information B.

This study has some limitations. The HN region is prone to inter and intra scan motion, even when patients are scanned with immobilization mask on the planning CT and MRI. Inter and intra scan motion makes it difficult to accurately register the synCT to the planCT. This can cause HU and dose differences that are not caused by an inaccurate synCT, but by residual misregistration and hence anatomical mismatch. Secondly, although the synCT generation model is trained on patients from multiple centers, it is only tested on patients from one center. Thirdly, the analysis of the accelerated scans was only performed on six scans. A larger number of accelerated ZTE scans should be analyzed to confirm our finding that the dose accuracy based on the 56 s ZTE-based synCT is indeed clinically acceptable. Finally, it should be noted that in addition to the ZTE scan a T1 and/or a T2 MRI is still needed for tumor and OAR delineations.

To conclude, this prospective study showed an excellent dosimetric accuracy for the clinical plans recalculated on ZTE-MR based synCT in the HN region. The ZTE scan be acquired in down to 56 s and is converted to a synCT using a multi-task 2D U-net. We also proposed a method to systematically assess dosimetric accuracy of synCT scans throughout the entire patient anatomy, using synthetic treatment plans and PTVs. We applied it and identified specific situations in which caution should be taken with very little beam angles, especially in more caudally located tumors. These situations were not picked up by the clinical plan comparison, which demonstrates the importance of using, in addition to clinical plans, synthetic plans to draw conclusions on dosimetric accuracy. This study is an important step towards clinical implementation of MR-only radiotherapy for HN cancer, using the silent and fast ZTE MRI.

## CRediT authorship contribution statement

**Iris Lauwers:** Writing – original draft, Visualization, Validation, Software, Methodology, Formal analysis, Data curation, Conceptualization. **Marta Capala:** Writing – review & editing, Supervision, Resources, Methodology, Funding acquisition, Conceptualization. **Sandeep Kaushik:** Writing – review & editing, Software, Resources, Methodology, Investigation, Data curation, Conceptualization. **László Ruskó:** Writing – review & editing, Methodology. **Cristina Cozzini:** Writing – review & editing, Software, Resources, Methodology, Investigation, Data curation, Conceptualization. **Jean-Paul Kleijnen:** Writing – review & editing, Methodology. **Jonathan Wyatt:** Writing – review & editing. **Hazel McCallum:** Writing – review & editing, Conceptualization. **Gerda Verduijn:** Writing – review & editing, Supervision, Resources. **Florian Wiesinger:** Writing – review & editing, Project administration, Methodology, Investigation, Funding acquisition, Data curation, Conceptualization. **Juan Hernandez-Tamames:**

Writing – review & editing, Resources, Methodology, Investigation, Funding acquisition, Data curation, Conceptualization. **Steven Petit:** Writing – original draft, Visualization, Validation, Supervision, Software, Project administration, Methodology, Investigation, Funding acquisition, Data curation, Conceptualization.

## Declaration of competing interest

The authors declare that they have no known competing financial interests or personal relationships that could have appeared to influence the work reported in this paper.

## Acknowledgments

This research is part of the Deep MR-only Radiation Therapy activity (project numbers: 19037, 20648, 210995) that has received funding from EIT Health. EIT Health is supported by the European Institute of Innovation and Technology (EIT), a body of the European Union and receives support from the European Union's Horizon 2020 Research and innovation program.

Erasmus MC Cancer Institute has research collaborations with Accuray Inc., Sunnyvale, USA, Elekta AB, Stockholm, Sweden and with Varian, a Siemens Healthineers Company (Palo Alto, CA, USA). Author IL acknowledges support from The Dutch Cancer Society (project number 12141).

## Appendix A. Supplementary data

Supplementary data to this article can be found online at https://doi.org/10.1016/j.radonc.2025.110762.

## References

[1] Boulanger M, Nunes JC, Chourak H, Largent A, Tahri S, Acosta O, et al. Deep learning methods to generate synthetic CT from MRI in radiotherapy: A literature review. Phys Med 2021;89:265–81.
[2] Johnstone E, Wyatt JJ, Henry AM, Short SC, Sebag-Montefiore D, Murray L, et al. Systematic Review of Synthetic Computed Tomography Generation Methodologies for Use in Magnetic Resonance Imaging-Only Radiation Therapy. Int J Radiat Oncol Biol Phys 2018;100:199–217.
[3] Karlsson M, Karlsson MG, Nyholm T, Amies C, Zackrisson B. Dedicated magnetic resonance imaging in the radiotherapy clinic. Int J Radiat Oncol Biol Phys 2009;74:644–51.
[4] McKenzie EM, Santhanam A, Ruan D, O'Connor D, Cao M, Sheng K. Multimodality image registration in the head-and-neck using a deep learning-derived synthetic CT as a bridge. Med Phys 2020;47:1094–104.
[5] Owrangi AM, Greer PB, Gilde-Hurst CK. MRI-only treatment planning: benefits and challenges. Phys Med Biol 2018;26.
[6] Spadea MF, Maspero M, Zaffino P, Seco J. Deep learning based synthetic-CT generation in radiotherapy and PET: A review. Med Phys 2021;48:6537–66.
[7] Lagendijk JJ, Raaymakers BW, van Vulpen M. The magnetic resonance imaging-linac system. Semin Radiat Oncol 2014;24:207–9.
[8] Du J, Carl M, Bydder M, Takahashi A, Chung CB, Bydder GM. Qualitative and quantitative ultrashort echo time (UTE) imaging of cortical bone. J Magn Reson 2010;207:304–11.
[9] Wiesinger F, Ho ML. Zero-TE MRI: principles and applications in the head and neck. Br J Radiol 2022;95:20220059.
[10] Palmer E, Karlsson A, Nordstrom F, Petruson K, Siversson C, Ljungberg M, et al. Synthetic computed tomography data allows for accurate absorbed dose calculations in a magnetic resonance imaging only workflow for head and neck radiotherapy. Phys Imaging Radiat Oncol 2021;17:36–42.
[11] Qi M, Li Y, Wu A, Lu X, Zhou L, Song T. Multisequence MR-generated sCT is promising for HNC MR-only RT: A comprehensive evaluation of previously developed sCT generation networks. Med Phys 2022;49:2150–8.
[12] Lerner M, Medin J, Jamtheim Gustafsson C, Alkner S, Olsson LE. Prospective Clinical Feasibility Study for MRI-Only Brain Radiotherapy. Front Oncol 2021;11:812643.
[13] Kaushik SS, Bylund M, Cozzini C, Shanbhag D, Petit SF, Wyatt JJ, et al. Region of interest focused MRI to synthetic CT translation using regression and segmentation multi-task network. Phys Med Biol 2023;68.
[14] Wiesinger F, Bylund M, Yang J, Kaushik S, Shanbhag D, Ahn S, et al. Zero TE-based pseudo-CT image conversion in the head and its application in PET/MR attenuation correction and MR-guided radiation therapy planning. Magn Reson Med 2018;80:1440–51.
[15] Wyatt JJ, Kaushik S, Cozzini C, Pearson RA, Petit S, Capala M, et al. Comprehensive dose evaluation of a Deep Learning based synthetic Computed Tomography algorithm for pelvic Magnetic Resonance-only radiotherapy. Radiother Oncol 2023;184:109692.
[16] Bambach S, Ho ML. Deep Learning for Synthetic CT from Bone MRI in the Head and Neck. AJNR Am J Neuroradiol 2022;43:1172–9.
[17] Ccmo. Deep learning based MR Only Radiotherapy for head-and-neck cancer. CCMO 2019.
[18] Engstrom M, McKinnon G, Cozzini C, Wiesinger F. In-phase zero TE musculoskeletal imaging. Magn Reson Med 2020;83:195–202.
[19] Wiesinger F, Sacolick LI, Menini A, Kaushik SS, Ahn S, Veit-Haibach P, et al. Zero TE MR bone imaging in the head. Magn Reson Med 2016;75:107–14.
[20] Korsholm ME, Waring LW, Edmund JM. A criterion for the reliable use of MRI-only. Radiat Oncol 2014;9.
[21] Bird D, Speight R, Andersson S, Wingqvist J, Al-Qaisieh B. Deep learning MRI-only synthetic-CT generation for pelvis, brain and head and neck cancers. Radiother Oncol 2024;191:110052.
[22] Dinkla AM, Florkow MC, Maspero M, Savenije MHF, Zijlstra F, Doornaert PAH, et al. Dosimetric evaluation of synthetic CT for head and neck radiotherapy generated by a patch-based three-dimensional convolutional neural network. Med Phys 2019;46:4095–104.
[23] Klages P, Benslimane I, Riyahi S, Jiang J, Hunt M, Deasy JO, et al. Patch-based generative adversarial neural network models for head and neck MR-only planning. Med Phys 2020;47:626–42.
[24] Olin AB, Hansen AE, Rasmussen JH, Ladefoged CN, Berthelsen AK, Hakansson K, et al. Feasibility of Multiparametric Positron Emission Tomography/Magnetic Resonance Imaging as a One-Stop Shop for Radiation Therapy Planning for Patients with Head and Neck Cancer. Int J Radiat Oncol Biol Phys 2020;108:1329–38.
[25] Olin AB, Thomas C, Hansen AE, Rasmussen JH, Krokos G, Urbano TG, et al. Robustness and Generalizability of Deep Learning Synthetic Computed Tomography for Positron Emission Tomography/Magnetic Resonance Imaging-Based Radiation Therapy Planning of Patients With Head and Neck Cancer. Adv Radiat Oncol 2021;6:100762.
[26] Scholey JE, Rajagopal A, Vasquez EG, Sudhyadhom A, Larson PEZ. Generation of synthetic megavoltage CT for MRI-only radiotherapy treatment planning using a 3D deep convolutional neural network. Med Phys 2022;49:6622–34.
[27] Singhrao K, Dugan CL, Calvin C, Pelayo L, Yom SS, Chan JW, et al. Evaluating the Hounsfield unit assignment and dose differences between CT-based standard and deep learning-based synthetic CT images for MRI-only radiation therapy of the head and neck. J Appl Clin Med Phys 2024;25:e14239.
[28] La Greca S-E, Dal Bello R, Lapaeva M, Fankhauser L, Pouymayou B, Konukoglu E, et al. Synthetic computed tomography for low-field magnetic resonance-only radiotherapy in head-and-neck cancer using residual vision transformers. Phys Imaging Radiat Oncol 2023;27:100471.